Spot Size Asymmetry in e-beam

February 1, 2018

Abstract

Measuring Spot Size Asymmetries with BPMs: There are 4 wire channels in a bpm. At present only 3 linear combinations of those channels are assessed to examine beam I,X,Y. There is a 4th linear combination which produces and independent variable which can be examined. This combination is proportional to the elliptical component of the spot size (aka the breathing mode).

1 BPM Position Measurement

The stripline beam position montiors (BPMs) consist of four wire antenna which each pickup an RF signal from the pulsed electron beam as it passes near the wires. The four wire channels are denoted X+ (xm), X- (xm), Y+ (yp), and Y- (ym). The signal each wire picks up is proportional to both e-beam intensity and the proximity of the e-beam to the wire in question. The raw signal from these wires is autogained typically, so that the magnitude of the DC converted channel signal is 3V and only small, fast deviations can be picked up by the DAQ.

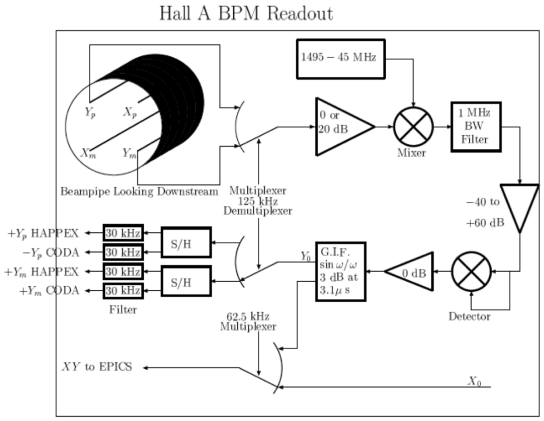

Figure 1: Schematic of the BPM readout electronics [1]

In the standard analysis, three combinations of the four wire channels are calculated: bpm x position, bpm y position, and bpm wire sum. The e-beam position is monitored directly by the calculated bpm x,y positions. Due to autogaining, the e-beam current is not directly monitored by the bpm wire sum, which only is used to assess fast, small changes such as charge asymmetry Aq. The mathematical manipulations in the analysis are as follows:

$$bpmx = \kappa(xp - xm)/(xp + xm) \tag{1}$$
$$bpmy = \kappa(yp - ym)/(yp + ym)$$
$$bpmws = xp + xm + yp + ym$$

Where κ is a stripline bpm calibration constant set to 18.76mm [2] [3]. The stripline antennas are either oriented along the hoziontal/vertical axes or they are oriented at $\pm 45^o$. Those that

are oriented along $\pm 45^o$ are rotated in analysis so that bpmx corresponds to horizontal and bpmy corresponds to vertical.

The signal from each antenna excited by the beam can be calculated [4] [5] as

$$S(\phi) = \beta \frac{I_{beam}}{2\pi} \frac{a^2 - r^2}{|\vec{a} - \vec{r}|^2} \tag{2}$$
$$= \beta \frac{I_{beam}}{2\pi} \frac{a^2 - r^2}{a^2 + r^2 - 2ar\cos(\phi - \theta)}$$

where a is the radius of BPM vacuum chamber, ϕ specifies the location of the bpm wire at $0, \pi/4, \pi/2, 3\pi/4$, r and θ specify the position of the electron beam, I_{beam} is the current of the electron beam, and β is a geometrical parameter which takes into account the finite thickness of the wire.

Using the difference/sum method, we can calculate the position of the beam as

$$bpmx = \kappa \frac{S(X+) - S(X-)}{S(X+) + S(X-)} = \kappa \frac{S(\phi = 0) - S(\phi = \pi)}{S(\phi = 0) + S(\phi = \pi)} \tag{3}$$
$$= \kappa \frac{2r\cos(\theta)}{a(1 + \frac{r^2}{a^2})} = \kappa \frac{2x}{a(1 + \frac{x^2+y^2}{a^2})} \approx \kappa \frac{2x}{a}$$
$$bpmx \approx \frac{a}{2} \frac{S(X+) - S(X-)}{S(X+) + S(X-)}$$

Hence for small r, the calibration constant $\kappa = a/2$. Phenomenologically, we observe in the Hall that $\kappa \approx$ 18.76mm-18.87mm [6] which means $a \approx$37.52mm-37.74mm.

For a gaussian current distribution of the electron beam, the signal for each antenna can be described as

$$S(\phi) = \int_0^{2\pi} \int_0^a r' dr' \beta \frac{j_{beam}(|\vec{r} - \vec{r'}|)}{2\pi} \frac{a^2 - r'^2}{|\vec{a} - \vec{r'}|^2} d\theta' \tag{4}$$
$$= \int_0^{2\pi} \int_0^a r' dr' \frac{\beta I_{beam}}{2\pi} \frac{e^{\frac{-|\vec{r} - \vec{r'}|^2}{2\sigma^2}}}{2\pi\sigma^2} \frac{a^2 - r'^2}{|\vec{a} - \vec{r'}|^2} d\theta'$$

This integral can be evaluated numerically for $\beta = 1$ and $I_{beam} = 1$ over the beam pipe area up to radius a, and a linear relationship is confirmed with calibration constant $\kappa \approx a/2$(Fig. 2).

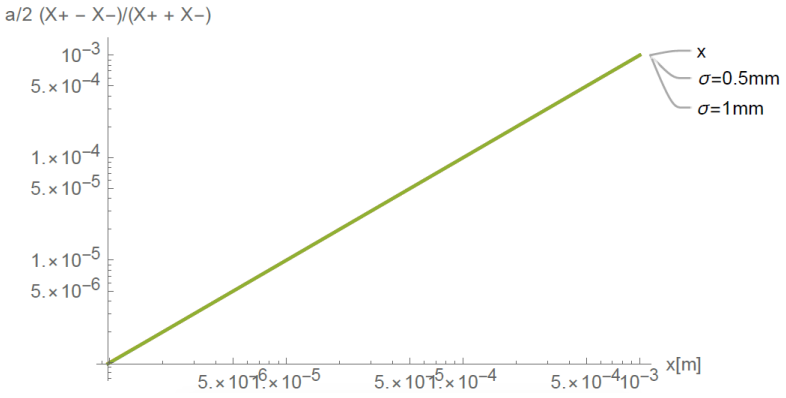

Figure 2: a

1.1 Pedestal Error

The charge asymmetry A_Q can couple to the measured position difference ΔX_M through a pedestal error. We define the pedestal error on each wire a ΔP_p and ΔP_m, the symmetric and asymmetric pedestals errors as $\Delta P_A = (\Delta P_p - \Delta P_m)/2$ and $\Delta P_S = (\Delta P_p + \Delta P_m)/2$, the radial distance to the wire as κ, and the wire sum as $W_S = X_p^A + X_m^A = I\alpha\kappa$ proportional to the beam current.

$$
\begin{aligned}
X^M &= \kappa \frac{X_p^M - X_m^M}{X_p^M + X_m^M} \\
&= \kappa \frac{X_p^A - X_m^A + \Delta P_p - \Delta P_m}{X_p^A + X_m^A + \Delta P_p + \Delta P_m} \\
&= \kappa \frac{X_p^A - X_m^A + 2\Delta P_A}{X_p^A + X_m^A + 2\Delta P_S} \\
&\approx X^A + 2\kappa \frac{\Delta P_A}{W_S} - 2X^A \frac{\Delta P_S}{W_S}
\end{aligned} \tag{5}
$$

The measured position difference can be calculated as

$$
\Delta X = X_0 - X_1 = X_0^A + 2\kappa \frac{\Delta P_A}{W_{S0}} - 2X_0^A \frac{\Delta P_S}{W_{S0}} - X_1^A - 2\kappa \frac{\Delta P_A}{W_{S1}} + 2X_1^A \frac{\Delta P_S}{W_{S1}} \tag{6}
$$

We note that

$$
\frac{1}{W_{S0}} - \frac{1}{W_{S1}} = \frac{1}{\alpha}\left(\frac{1}{I + \Delta I} - \frac{1}{I - \Delta I}\right) = \frac{1}{\alpha I}(1 - \Delta I/I - 1 - \Delta I/I) \approx \frac{-2A_Q}{W_S} \tag{7}
$$

Hence,

$$
\Delta X^M = \Delta X^A \left(1 + \frac{2\Delta P_S}{W_S}\right) + 4X^A A_Q \frac{\Delta P_S}{W_S} - 4\kappa A_Q \frac{\Delta P_A}{W_S} \tag{8}
$$

A 5% asymmetric pedestal error could result in a coupling of 4nm/ppm. For nostalgic purposes we also include a transparency astutely created by a postdoc in the early 2000's Fig. 3)

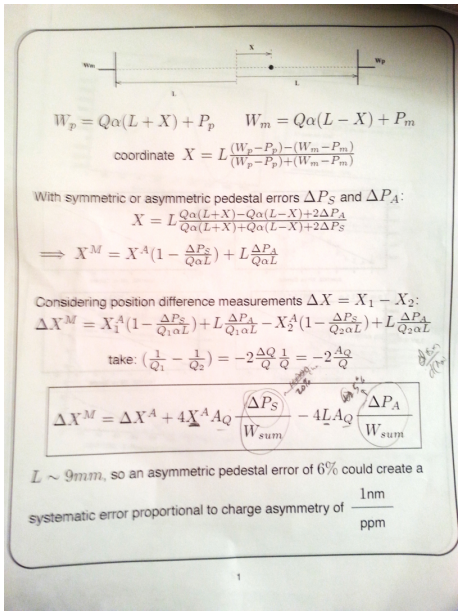

Figure 3

2 BPM Spot Size Asymmetry Measurement

There are four bpm wire channels, yet only three parameters have been calculated from them in the standard analysis. A fourth parameter can be calculated: the spot size asymmetry A_σ. There are several ways to describe spot-size, but we could model it as having a circular σ_{circ} component and and an elliptical component $\epsilon \approx (\sigma_x - \sigma_y)/(\sigma_x + \sigma_y)$. The spot size can be described as $\sigma(\theta) = \sigma_{circ} + \epsilon\cos(2(\theta - \theta_i))$, where θ is the angle in the plane transverse to the direction of beam propagation. Depending on the orientation of the wire channels and the orientation of the electron beam, a given bpm may be sensitive to ϵ or insensitive to it. Likewise we can describe spot size asymmetry as $A_\sigma(\theta) = A_{circ} + A_{elli}\cos(2(\theta - \theta_0))$, where the elliptical term is what we refer to

as the 'breathing mode' of the spot size asymmetry. A_{elli} can be related to a difference in ϵ via $Aelli \approx (\epsilon_0 - \epsilon 1)/(\sigma_0 + \sigma 1) \approx \Delta\epsilon/2 \approx (\epsilon_0/\sigma_0 - \epsilon_1/\sigma_1)/2$. A_{circ} is also an important parameter which we are also sensitive to in a bpm, but it manifests itself similarly to A_Q and we cannot distinguish a separate entity (unless perhaps a bpm and bcm are in very close proximity in the beamline). So, in this analysis, we focus on the elliptical term of the spot size asymmetry.

Using the bpm wire channels we can obtain information about the elliptical component of the spot size asymmetry A_{elli} .

$$bpmelli = \frac{a^2(xp + xm - yp - ym)}{8\sigma^2(xp + xm + yp + ym)} \tag{9}$$

$$\epsilon = bpmelli - bpmecorr = \frac{a^2(xp + xm - yp - ym)}{8\sigma^2(xp + xm + yp + ym)} - f(x_0, y_0) \approx \frac{\sigma_x - \sigma_y}{\sigma_x + \sigma_y}$$

where $a \approx 2\kappa = 37.52mm$ the radius of BPM vacuum chamber, σ is the e^-beam spot size, and $f(x_0, y_0)$ is a correction term related to the position of the electron beam.

2.1 Derivation of bpmelli

The above equation is an approximation derived from numerical integration. For a gaussian current distribution of the electron beam centered at (x_0,y_0) relative to the center of the beamline at $r = 0$, the signal for each antenna can be described as

$$S(\phi) = \int_0^a d\Delta r \int_0^{2\pi} d\theta' \Delta r I_{beam} e^{-\frac{(\Delta r\cos(\theta') - x_0)^2}{2\sigma_x^2} - \frac{(\Delta r\sin(\theta') - y_0)^2}{2\sigma_y^2}} \frac{a^2 - \Delta r^2}{4\pi^2\sigma_x\sigma_y(a^2 + \Delta r^2 - 2a\Delta r\cos(\theta' - \phi))} \tag{10}$$

$$S(X\pm) \approx \int\int dxdy I_{beam} e^{-\frac{(x-x_0)^2}{2\sigma_x^2} - \frac{(y-y_0)^2}{2\sigma_y^2}} \frac{a^2 - x^2 - y^2}{4\pi^2\sigma_x\sigma_y((a \mp x)^2 + y^2)}$$

$$S(Y\pm) \approx \int\int dxdy I_{beam} e^{-\frac{(x-x_0)^2}{2\sigma_x^2} - \frac{(y-y_0)^2}{2\sigma_y^2}} \frac{a^2 - x^2 - y^2}{4\pi^2\sigma_x\sigma_y(x^2 + (a \mp y)^2)}$$

For a centered electron beam at (x_0,y_0)=(0,0), for each wire location, this integral can be evaluated numerically over the circular area centered on the beamline up to radius a, the bpm chamber radius Normalizing the result to $a^2/\sigma^2/8$, we obtain the elliptical spot size term $\epsilon = \frac{\sigma_x - \sigma_y}{\sigma_x + \sigma_y}$ (Fig. 4). We note that this normalization is largely to correct σ dependence in the numerator xp+xm-yp-yp as opposed to the denominator xp+xp+yp+ym which is not very sensitive to σ (the wire sum only changes <0.1% over the range 200um< σ <2mm, whereas the numerator changed by over an OOM).

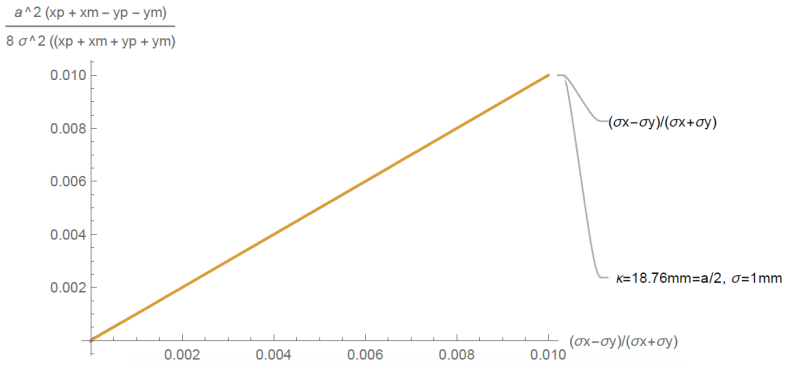

Figure 4

2.2 Position Dependence of bpmelli

Regarding the dependence of bpmelli on beam position, this integral is highly dependent on the position of the electron beam (x_0,y_0). We set $\epsilon = 10^{-4}$ and evaluate bpmelli for several beam positions (Fig. 5). We observe that there is a large correction term to bpmelli, proportional to

the square of the distance from the beamline, approximately $f(x_0, y_0) = g1\frac{x_0^2 - y_0^2}{\sigma^2} - g2\frac{x_0^4 - y_0^4}{\sigma^2}$, where $g1 = 0.250014$ and $g2 = 2.84739m^{-2}$ when evaluated for $a = 2\kappa$, $\kappa = 18.76mm$, $\sigma = 1mm$.

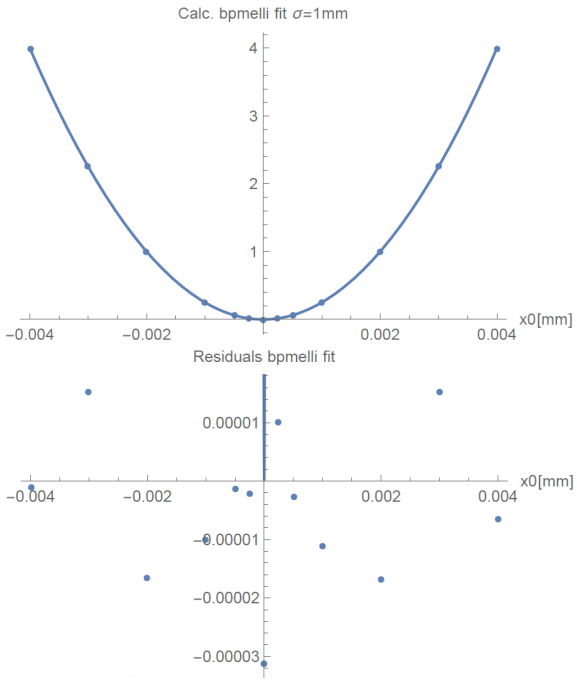

Figure 5

However, when we evaluate small differences in ϵ, letting $\Delta\epsilon = 10^{-4}$, even far from the beamline center, diff_bpmelli is still accurate, whether the beam is a $x_0 = 0$ or at $x_0 = 8mm$ (Fig. 6). So, we should expect that the calculated raw ellipticity will vary with beam position, but the pair-wise asymmetry in that ellipticity will still be approximately correct.

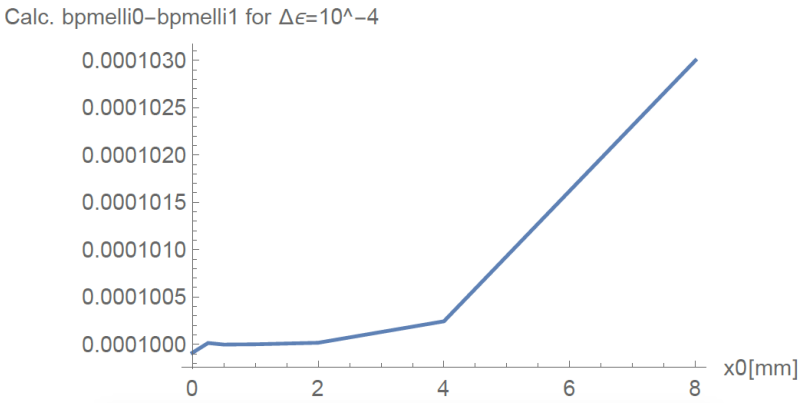

Figure 6

2.3 Antenna Sensitivity to 0th, 1st, and 2nd moments

We evaluate the antenna signal response to the presence of current $\delta S(r, \phi, \theta) = \beta\frac{\delta I_{beam}}{2\pi}\frac{a^2 - r^2}{a^2 + r^2 - 2ar\cos(\phi - \theta)}$ with respect to x. Evaluating the 1st and 2nd derivatives $\frac{d\delta S(r,\phi,\theta)}{dr}$ and $\frac{d^2\delta S(r,\phi,\theta)}{dr^2}$ for $\beta\delta I_{beam} = 1$, $\phi = 0$(examining the X+ wire), $\theta = 0$(moving along x direction), we obtain the sensitivity of the wire signal to the 0th, 1st and 2nd moments, seeing that each moment decreases by an order of magnitude (Fig. 7).

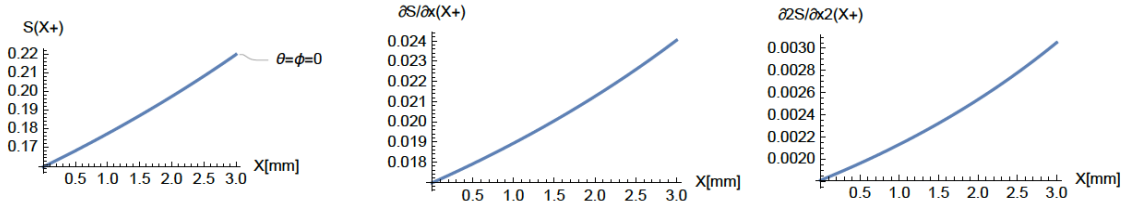

Figure 7

2.4 Pedestal Error in bpmelli

The charge asymmetry A_Q and the radial spot size asymmetry A_{circ} can couple to the measured elliptical spot size asymmetry $A_{elli} = \Delta\epsilon$ through a pedestal error. We define the pedestal error on the x-wires and y-wires as $\Delta P_{Sx} = (\Delta P_{xp} + \Delta P_{xm})/2$ and $\Delta P_{Sy} = (\Delta P_{yp} + \Delta P_{ym})/2$, the symmetric and asymmetric pedestals errors as $\Delta P_A = \Delta P_{Sx} - \Delta P_{Sy}$ and $\Delta P_S = \Delta P_{Sx} + \Delta P_{Sy}$, the radial distance to the wire as a, and the wire sum as $W_S = X_p^A + X_m^A + Y_p^A + Y_m^A = I\alpha\sigma$ proportional to the beam current and spot-size.

$$\begin{aligned}
\epsilon^M &= \frac{a^2}{8\sigma^2}\frac{X_p^M + X_m^M - Y_p^M - Y_m^M}{X_p^M + X_m^M + Y_p^M + Y_m^M} \qquad (11)\\
&= \frac{a^2}{8\sigma^2}\frac{X_p^A + X_m^A - Y_p^A - Y_m^A + \Delta P_{xp} + \Delta P_{xm} - \Delta P_{yp} - \Delta P_{ym}}{X_p^A + X_m^A + Y_p^A + Y_m^A + \Delta P_{xp} + \Delta P_{xm} + \Delta P_{yp} + \Delta P_{ym}}\\
&= \frac{a^2}{8\sigma^2}\frac{X_p^A + X_m^A - Y_p^A - Y_m^A + 2\Delta P_A}{X_p^A + X_m^A + Y_p^A + Y_m^A + 2\Delta P_S}\\
&\approx \epsilon^A + 2\frac{a^2}{8\sigma^2}\frac{\Delta P_A}{W_S} - 2\epsilon^A\frac{\Delta P_S}{W_S}
\end{aligned}$$

The measured elliptical spot-size asymmetry can be calculated as

$$A_{elli}^M = \frac{1}{2}\Delta\epsilon^M = \frac{1}{2}(\epsilon_0 - \epsilon_1) = \epsilon_0^A/2 + \frac{a^2}{8\sigma^2}\frac{\Delta P_A}{W_{S0}} - \epsilon_0^A\frac{\Delta P_S}{W_{S0}} - \epsilon_1^A/2 - \frac{a^2}{8\sigma^2}\frac{\Delta P_A}{W_{S1}} + \epsilon_1^A\frac{\Delta P_S}{W_{S1}} \qquad (12)$$

We note that

$$\frac{1}{W_{S0}} - \frac{1}{W_{S1}} = \frac{1}{\alpha}(\frac{1}{I_0} - \frac{1}{I_1}) = \frac{1}{\alpha}(\frac{1}{I + \Delta I} - \frac{1}{I - \Delta I}) \approx -\frac{2A_Q}{W_S} \qquad (13)$$

Hence,

$$A_{elli}^M = \frac{1}{2}\Delta\epsilon^M = A_{elli}^A(1 + \frac{2\Delta P_S}{W_S}) + 2\epsilon^A A_Q\frac{\Delta P_S}{W_S} - 2\frac{a^2}{8\sigma^2}A_Q\frac{\Delta P_A}{W_S} \qquad (14)$$

For $a = 2\kappa$,$\kappa = 18.76mm$ and $\sigma = 1.5mm$, for a 5% asymmetric pedestal error the false elliptical spot size asymmetry is $7.8 \times 10^-6/ppm$ for A_Q. To test this equation, we can induce a 5% asymmetric pedestal error in our analysis. The wire sum signal is 3e4 channels on the vqwk ADCs. Applying 3000ch to the pedestals of xp and xm, and -3000ch to yp and ym, we obtain a 5% asymmetric pedestal error. The slope observed in the first 8 bpms in a PITA scan (Run3338), shows a coupling between A_{elli} and A_Q of $6.4 - 7.6 \times 10^-6/ppm$, consistent with our calculated pedestal error value.

2.5 Position Difference Error in bpmelli

The position sensitivity correction term in bpmelli, which we now define as bpmecorr, was found to be approximately

$$bpmecorr = f(x,y) = g1\frac{x^2 - y^2}{\sigma^2} - g2\frac{x^4 - y^4}{\sigma^2} \qquad (15)$$

where $g1 = 0.250014$ and $g2 = 2.84739m^{-2}$. We evaluate how this position dependence leads to coupling between position differences and measured A_{elli}.

$$\Delta bpmecorr = \Delta f(x,y) = f(x0,y0) - f(x1,y1) = g1\frac{x_0^2 - y_0^2}{\sigma^2} - g1\frac{x_1^2 - y_1^2}{\sigma^2} - g2\frac{x_0^4 - y_0^4}{\sigma^2} + g2\frac{x_1^4 - y_1^4}{\sigma^2} \tag{16}$$

$$\approx 0.25\frac{4x\Delta x - 4y\Delta y}{\sigma^2} - 2.84m^{-2}\frac{8x^3\Delta x + 8\Delta x^3 x}{\sigma^2} \approx \frac{x\Delta x - y\Delta y}{\sigma^2}$$

We note the x^4 term is negligible in the mm regime. The coupling between position difference Δx and $\Delta\epsilon$, for $\sigma = x = 1mm$, is $10^{-6}/nm$, which may or may not be significant depending on the size of the position differences and the size of the spot size asymmetry your trying to measure. However, for a more extreme case, $\sigma = 0.5mm$ and $x = 10mm$, the coupling is $4e-5/nm$, which for 50nm position differences gives false $\Delta\epsilon$ of up to 2×10^{-3}. We can eliminate this dependence approximately in analysis by subtracting the correction term bpmecorr from bpmelli : $A_{elli} \approx \Delta\epsilon/2 \approx$ diff_bpmelli/2-diff_bpmecorr/2.

2.6 Spot size scale factor error

It is possible that our estimates of spot-size are different from the actual beam spot size at a given bpm. This can affect both our measured diff_bpmelli, diff_bpmecorr and Aelli. The error is a scale factor given by the square of the ratio of actual beam size to applied beam size.

$$\Delta bpmecorr^A \approx \frac{x\Delta x - y\Delta y}{(\sigma^A)^2} = (\frac{\sigma^M}{\sigma^A})^2 \Delta bpmecorr^M \tag{17}$$

$$\Delta\epsilon^A = (\frac{\sigma^M}{\sigma^A})^2 \Delta\epsilon^M \tag{18}$$

$$A_{elli}^A = \frac{1}{2}(\Delta\epsilon^A - \Delta bpmecorr^A) = (\frac{\sigma^M}{\sigma^A})^2 A_{elli}^M \tag{19}$$

$$scalef = (\frac{\sigma^M}{\sigma^A})^2 \tag{20}$$

2.7 Applying bpmelli in Data Analysis

We analyze our best run of 2017 with the RTP cell, which had 100nm position differences in the injector. We also analyze a subsequent run with an aligned KD*P cell immediately following, which had the same injector setup. These runs are in the 100keV portion of the injector and cover bpms: 1I02,1I04,1I06,0I01,0I01A,0I02,0I02A, and 0I05.

2.7.1 Determining σ

We introduced bpmelli into our standard analysis, pan, treating $a = 2\kappa$, $\kappa = 18.76mm$ and $\sigma = 1.5mm$. The reasoning behind this choice of σ includes laser measurements and e-beam optics simulation. The laser spot size on the cathode during August 2017 was measured to be $\sigma = 0.75mm$. Examining Elegant (Fig. 8), the beamline simulation software used by the accelerator, if the initial σ is 0.25mm, then for the first 8 bpms in the injector the spot size σ is between 0.4mm and 0.6mm, assuming the model in Elegant is correct. If we scale our measured cathode spot size using Elegant, it is reasonable to assume $1.2mm < \sigma < 1.8mm$ in the 100keV injector region. Applying a fixed σ is not strictly correct for all bpms since the beam size changes throughout the accelerator, and we expect a $\pm 25\%$ scale error in the 100keV region.

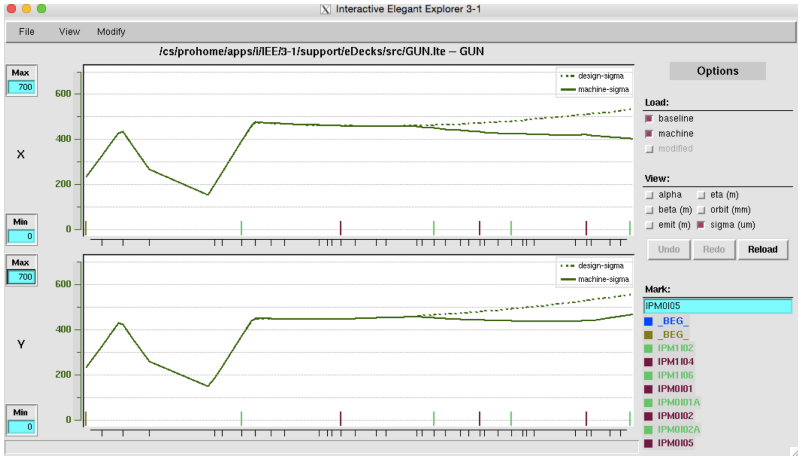

Figure 8

Further downstream in the injector, ELEGANT predicts the spot-size changing more significantly.

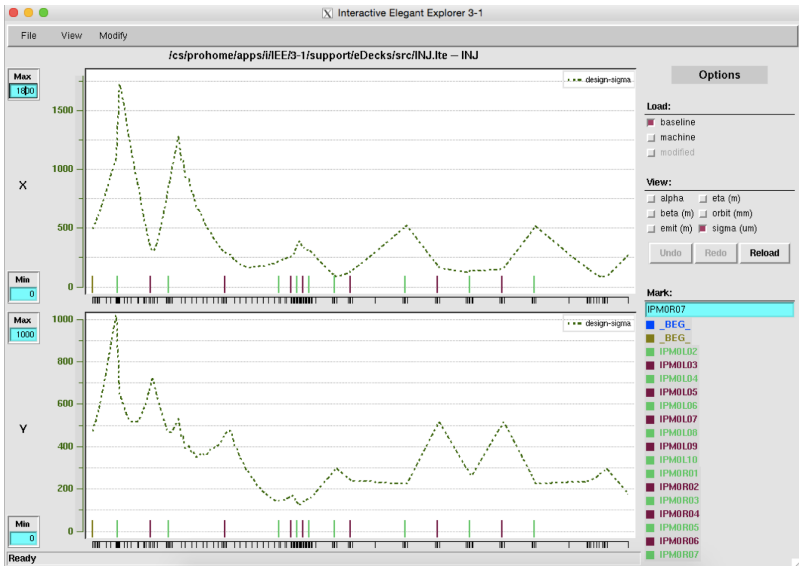

Figure 9

2.7.2 Checking Pedestal Error - RTP

To check the pedestals, we examine a PITA scan in the RTP (Run3338). The couplings between diff_bpmelli and Aq as measured by the PITA scan are small and vary in sign, $\frac{d\Delta\epsilon}{dAq}$ between -5×10^{-7}/ppm and 3×10^{-7}/ppm, indicating small pedestal errors. For comparison, when pedestal errors of 5% are intentionally induced, the slopes are much larger, 1.3×10^{-5}/ppm-1.5×10^{-5}/ppm, and all have the same sign for all 8 bpms. This indicates that our pedestal errors are extremely small.

The same analysis was performed for the PITA scan in the KD*P data (Run3444). The couplings between diff_bpmelli and Aq as measured by this PITA scan are also small and vary in sign, $\frac{d\Delta\epsilon}{dAq}$ between -7×10^{-7}/ppm and 3×10^{-8}/ppm, indicating small pedestal errors for the KD*P data as well.

2.7.3 Checking Couplings to PITAposU/V - RTP

With the RTP cell, we have the advantage of being able to perform PITAposU/V scans which allow us to control the position differences and examine the couplings between diff_bpmelli and diff_bpmecorr and these position differences, as well as examine any sensitivity of Aelli to PITA

posU/V. The position difference sensitivity of diff_bpmelli and diff_bpmecorr should be very similar, since the purpose of diff_bpmecorr to correct position difference sensitivity when we subtract it out Aelli=(diff_bpmelli-diff_bpmecorr)/2. Any residual correlation of Aelli to PITAposU/V must be due Aelli actually changing as we vary the voltage.

The position difference sensitivity of diff_bpmecorr is expected to be x/σ^2 where x is the deviation of the beam from center, which for these runs was ±4mm or so, and σ is the spot size used, which for this analysis was 1.5mm. So we expect a position difference sensitivity in the range of $\frac{d\Delta\epsilon}{d\Delta x} \approx \pm 1.8 \times 10^{-6}$/nm. Examining the tables of the slopes from PITAposU/V scans below (Fig. 10 , Fig. 11) , that is exactly what we observe in diff_ecorr vs Dx,Dy.

	Aelli vs PITAposU	Delli vs Dx(nm)	Decorr vs Dx(nm)	Aelli vs Dx(nm)
1I02	-4.9E-07	-1.0E-06	-1.2E-06	9.0E-08
1I04	1.6E-06	-6.1E-08	-4.8E-07	2.1E-07
1I06	-1.4E-06	3.3E-08	3.3E-07	-1.5E-07
0I01	-7.6E-07	1.2E-08	3.2E-07	-1.5E-07
0I01A	6.0E-07	-5.0E-07	-1.3E-06	4.0E-07
0I02	-1.0E-06	2.2E-07	3.6E-08	9.5E-08
0I02A	4.0E-06	4.9E-07	9.4E-07	-2.2E-07
0I05	1.3E-05	-2.5E-07	-4.0E-07	7.6E-07

Figure 10: Run3339 PITAposU table

	Aelli vs PITAposV	Delli vs Dy(nm)	Decorr vs Dy(nm)	Aelli vs Dy(nm)
1I02	2.9E-06	1.2E-06	2.5E-06	-6.5E-07
1I04	-5.1E-07	3.5E-06	4.3E-07	1.5E-06
1I06	-2.6E-06	4.5E-07	1.2E-06	-3.8E-07
0I01	1.0E-07	3.5E-07	2.4E-07	5.8E-08
0I01A	-1.1E-06	2.2E-07	-9.6E-07	5.9E-07
0I02	7.2E-08	1.7E-07	1.9E-07	-6.2E-09
0I02A	-4.8E-06	-1.0E-06	-1.6E-06	2.8E-07
0I05	4.1E-06	-4.7E-07	-1.1E-06	3.0E-07

Figure 11: Run3339 PITAposV table

It is also important to know how Aelli is affected by PITAposU/V. Since we use these voltages to minimize position differences, it is important that in doing so, we are not increasing spot-size asymmetry significantly. The largest slope observed in the 100keV region is $1.3e-5$/V in 0I05. That means changing PITAposU/V by 10V may change Aelli by 10^-4 in 0I05. The position difference control in 0I05 was 17nm/V. So, put another way, using PITAposU/V to correct a position difference of 130nm in 0I05 may change Aelli by 10^{-4}. These sensitivities can be verified or refuted by actual laser table measurements with the linear array. It should be noted that our choice of PITAposU/V voltages to zero position differences may also come close to the zero of spot-size asymmetries, since even though we applied PITAposU=12.69V, PITAposV=70.98V to get <100nm position differences, as shown in the next section, Aelli was still bounded as $<10^{-4}$.

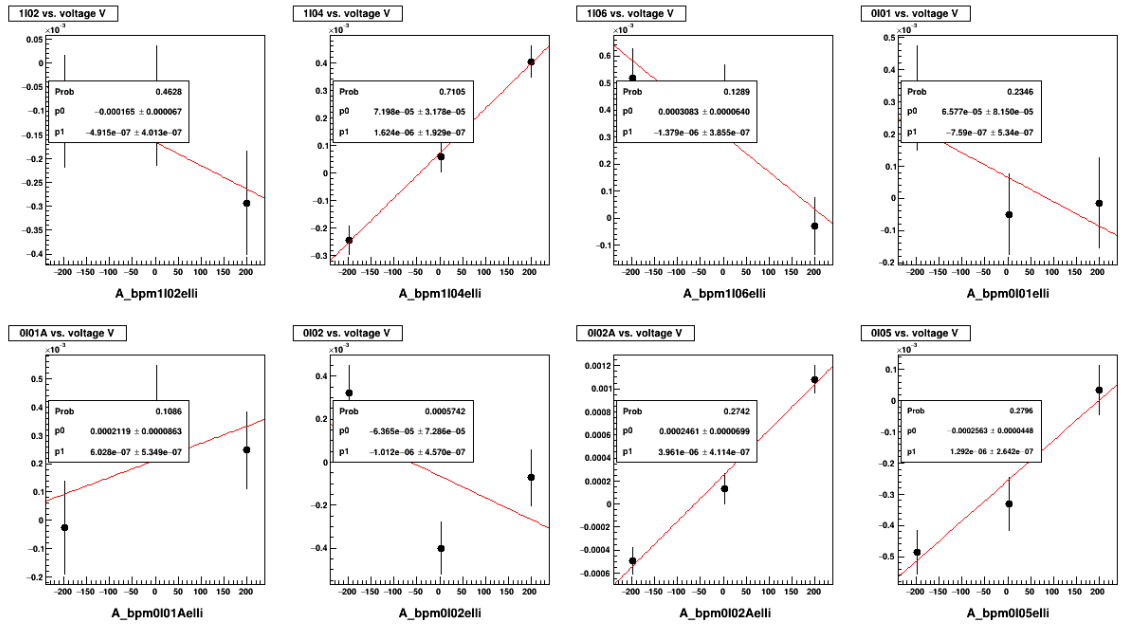

Figure 12: 3339 PITAposU scan

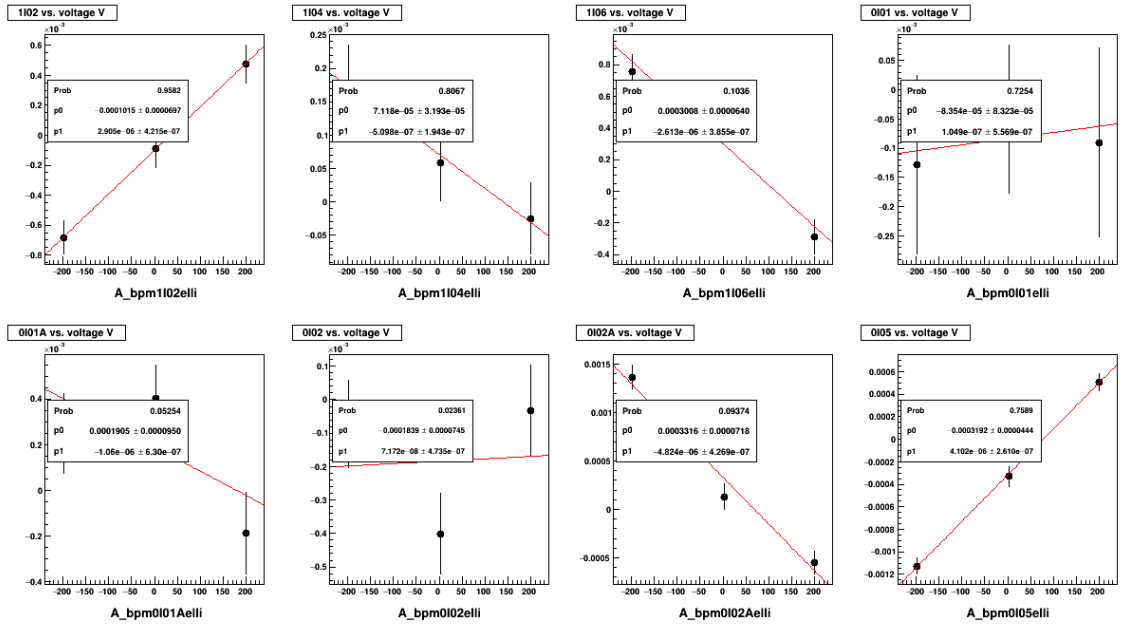

Figure 13: Run3339 PITAposVscan

2.7.4 e-beam rotation and scale-factor error

PITA pos U and V scans with the RTP allow us to assess what is happening rotationally to the electron beam, as well as identify any nodes in the propagation. In performing a PITAposU scan, we make the position differences of a known size along -45^o on the laser table. By examining the position difference observed in each bpm, we can see if the the position difference remains along -45^o or if it is rotated (i.e. the observed position difference is along only the horizontal, for example). Additionally, if we know we've induced a 1um position difference at the cathode and yet we only observe 100nm at a given bpm, we know that the e-beam is going through a node in the optics of the injector. We can observe that the first bpm in the beamline 1I02 sees position differences from PITAposU along -48^o, so the e-beam at 1I02 is not rotated relative to the laser table orientation. However, for these injector settings, the subsequent bpms 1I04-0I05 see position differences from PITAposU mainly along $\approx 0^o$, the horizontal, indicating the e-beam is rotated

by 45^o relative to the laser orientation. That means if we have an elliptical spot size asymmetry along the x/y on the laser table, we'll see it in bpm1I02 which has it's wire channels along x/y and where the e-beam has the same orientation as the laser, but not is subsequent bpms. And if we have an elliptical spot size asymmetry along u/v on the laser table (ie the diagonal), we'll see it in bpms 1I04-0I05 which have their wire channels along x/y and where the e-beam is rotated 45^o relative to the laser, but not in 1I02.

		Couplings before solenoid flip IHWP out, S1, Run3339		Est. from Dr	(1.5mm)^2/sigma^2
		PITAposU (-45deg)	PITAposV (+45deg)	sigma(mm)	scale factor error
Dr ~ laser	nm/V	7.09	5.72	0.75	4.00
theta laser	deg	-47.96	32.97		
Dr 1I02	nm/V	6.27	5.25	0.67	4.95
theta 1I02	deg	29.20	-58.56		
Dr 1I04	nm/V	7.81	7.79	0.91	2.70
theta 1I04	deg	7.86	-85.67		
Dr 1I06	nm/V	9.42	6.89	0.96	2.47
theta 1I06	deg	9.55	89.96		
Dr 0I01	nm/V	5.01	1.84	0.40	14.00
theta 0I01	deg	8.44	77.63		
Dr 0I01A	nm/V	1.54	2.10	0.21	49.45
theta 0I01A	deg	12.94	-70.08		
Dr 0I02	nm/V	10.64	12.08	1.33	1.27
theta 0I02	deg	0.91	-83.86		
Dr 0I02A	nm/V	17.62	17.26	2.04	0.54
theta 0I02A	deg	1.34	-80.78		
Dr 0I05	nm/V	17.16	13.55	1.80	0.70
theta 0I05	deg	6.68	89.50		

Figure 14: Couplings Angles 3339

Examining the radial position differences per PITA pos V ($\frac{dDr}{dV}$) in 0I01 and 0I01A, we see only 1-2nm/V at those bpms, when the laser at the cathode was estimated to have 6nm/V. This suppression of position differences sensitivity indicated a node in the e-beam optics. Examining 0I02 and 0I05, we see sensitivities like 17nm/V indicating an expansion in the e-beam optics. If the injector were viewed as simply a series of lenses were the beam were centered, from an entirely ray optics perspective, these sensitivities to motion would scale with beam size. In an overly simplified model, the $\frac{dDr_{bpm}}{dDr_{laser}} \approx \sigma_{bpm}/\sigma_{laser}$. We can use PITAposU/V scans to check for errors in the Elegant simulation and errors in our assumption of $\sigma = 1.5$mm at the bpms. We know the laser spot size at the cathode is 0.75mm. Estimating the e-beam spot size from Dr sensitivity, we see spot-sizes in the range 0.2mm-2mm. Of course, at nodes, the ray-optics model breaks down, so we shouldn't use this model for bpms 0I01 and 0I01A. For the other bpms, we estimate a scale-factor error, discussed in a previous section, which could potentially be applied to Aelli via $A^A_{elli} = scalefA^M_{elli} = (\frac{\sigma^M}{\sigma^A})^2 A^M_{elli}$. These scale-factor corrections are estimated in this ray-optics model to be anywhere from 0.5X-5X. It should be noted that these numbers should be taken lightly, only used for qualitative explanations and not quantitative interpretations. (We note the laser position difference control at the cathode is estimated from the quadphotodiode measurement using throw distance to the cathode 2.014m and the throw to the qpd 1.04m).

2.7.5 RTP and KD*P best-case runs

The analysis of the best case RTP run indicates position differences <100nm and elliptical spot size asymmetries Aelli=(diff_bpmelli-diff_bpmecorr)/2 on the order of 10^{-4} (Fig. 15 , in black). diff_bpmelli is also shown in green and the systematic error contribution diff_bpmecorr from the beam not being centered on a given bpm is also shown in red, and they are on a similar order to the spot size asymmetry. The systematic error contribution from Aq (<5ppm) through pedestal error coupling, found to be $< 10^{-6}$/ppm from the PITA scan, must be $< 5 \times 10^{-6}$ and is therefore negligible. This measurement appears to bound the elliptical spot size asymmetry as being $<10^-4$ both along x/y (bpm 1I02) and along u/v (bpms 1I04-0I05), as discussed in the e-beam rotation section above.

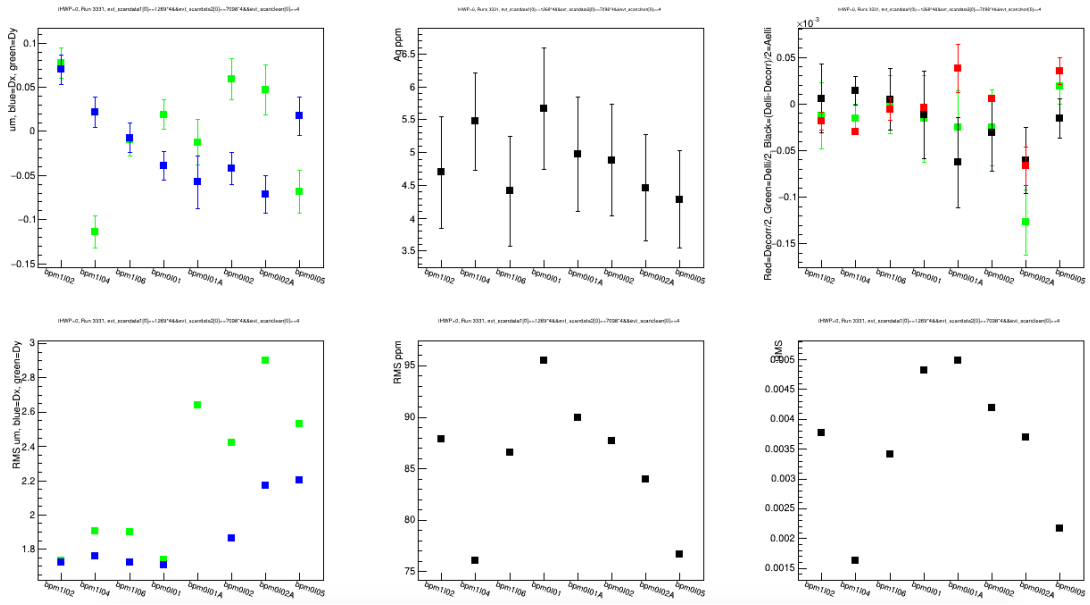

Figure 15: RTP cell Run3331 withbpmelli

The KD*P cell shows position differences <200nm adn elliptical spot size asymmetries slightly larger than for the RTP, on the order of 2×10^{-4} (Fig. 16). The systematic error from diff_bpmecorr is comparable to what it was for the RTP $< 10^{-4}$ (shown in red). The systematic error contribution from Aq (<5ppm) through pedestal error coupling is negligble as it was for RTP.

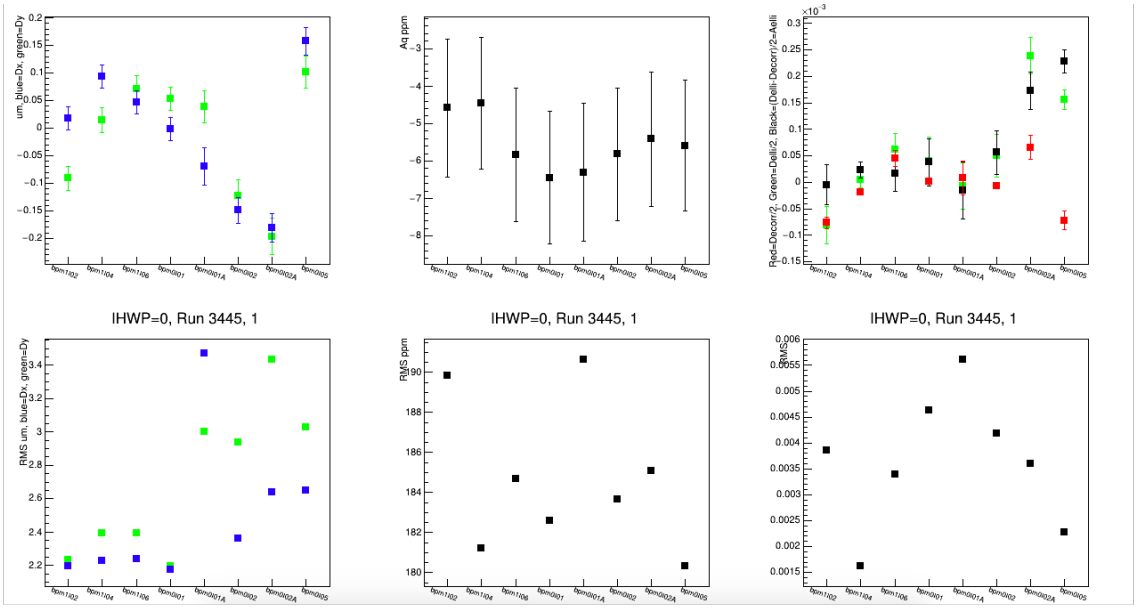

Figure 16: KDP Run3445 bestcase withbpmelli

This systematic error $\Delta bpmecorr$ is from the fact that the e-beam isn't centered on some of the bpms; it is up to 4mm off center. The larger the deviation from the beam being centered, the greater the systematic error contribution to $A_{elli} = \frac{1}{2}(\Delta bpmelli - \Delta bpmecorr)$. We determined from PITAposU/V scans that the contribution for the RTP expected to be x/σ^2 was $< 2 \times 10^{-6}$/nm. The beam positions x,y for each bpm are shown below (Fig. 17 (a)) and are on the order of $\pm 3mm$ for both the RTP run and KD*P run (Fig. 17 (b)) and look almost identical.

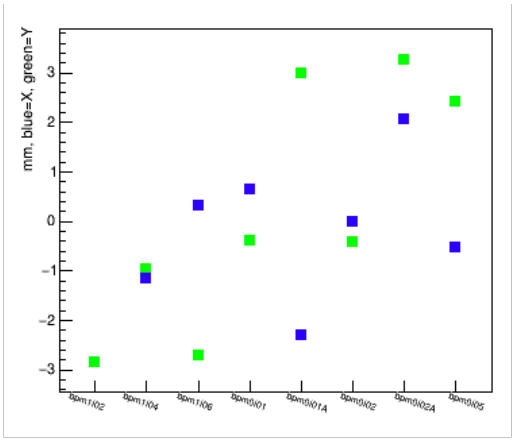

(a) Run3331 RTP XY

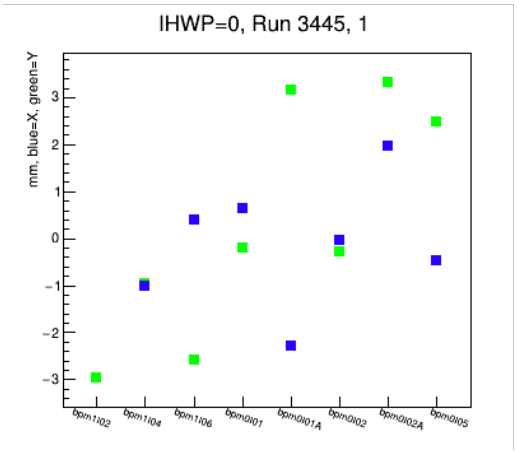

(b) KD*P Run3445 XY

Figure 17: beam XY positions along beamline

2.7.6 RTP and KD*P runs with scale-factor applied

We can redo the best-case run plots assuming our 1.5mm for spot size in not correct and using the potential scale-factor errors we derived from the PITA pos U/V scans above. Scaling Aelli by these potential scale factor errors produces the following plot for scaled-Aelli in RTP (Fig. 18 (a)) and KD*P (Fig. 18 (b)).

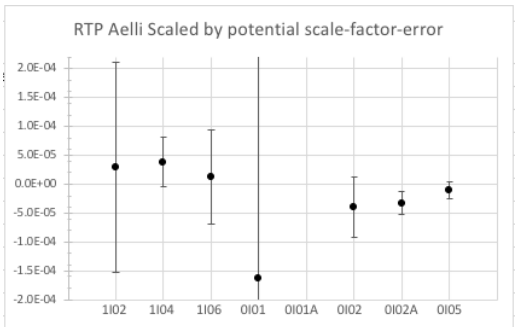

	Aelli	Aelli error	scale factor error	Aelli scaled	Aelli scdl. err
bpm1I02	5.9E-06	3.7E-05	5.0	2.9E-05	1.8E-04
bpm1I04	1.4E-05	1.6E-05	2.7	3.8E-05	4.2E-05
bpm1I06	4.9E-06	3.3E-05	2.5	1.2E-05	8.1E-05
bpm0I01	-1.2E-05	4.7E-05	14.0	-1.6E-04	6.5E-04
bpm0I01A	-6.3E-05	4.8E-05	49.4	-3.1E-03	2.4E-03
bpm0I02	-3.1E-05	4.1E-05	1.3	-4.0E-05	5.2E-05
bpm0I02A	-6.1E-05	3.6E-05	0.5	-3.3E-05	1.9E-05
bpm0I05	-1.6E-05	2.1E-05	0.7	-1.1E-05	1.5E-05

(a) Run3331 RTP Aelli Scaled

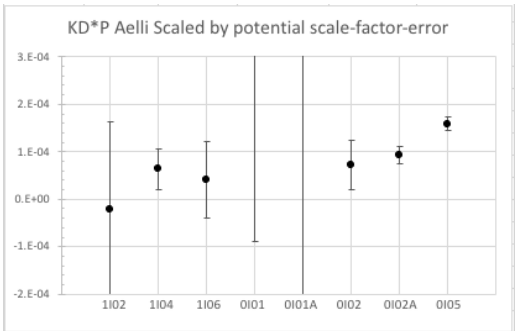

	Aelli	Aelli error	potential scale factor error	Aelli scaled	Aelli scdl. err
bpm1I02	-4.3E-06	3.7E-05	5.0	-2.1E-05	1.8E-04
bpm1I04	2.4E-05	1.6E-05	2.7	6.4E-05	4.2E-05
bpm1I06	1.6E-05	3.3E-05	2.5	4.0E-05	8.1E-05
bpm0I01	3.8E-05	4.5E-05	14.0	5.4E-04	6.3E-04
bpm0I01A	-1.6E-05	5.4E-05	49.4	-7.7E-04	2.7E-03
bpm0I02	5.6E-05	4.1E-05	1.3	7.2E-05	5.2E-05
bpm0I02A	1.7E-04	3.5E-05	0.5	9.3E-05	1.9E-05
bpm0I05	2.3E-04	2.2E-05	0.7	1.6E-04	1.5E-05

(b) Run3445 KD*P Aelli Scaled

Figure 18: Aelli scaled by scale factor error $(\sigma^A/\sigma^{est})^2$ estimated from position difference sensitivity to PITAposU/V scans

The scale-factors for 0I01 and 0I01A are very large and we discount them because those bpms are at a node where the simplistic ray-optics model these factors were dervied from breaks down. Examining bpm1I02, which is sensitive to elliptical asymmetries along x/y laser table coordinates, Aelli is bounded as $< 2 \times 10^{-4}$. Examining bpm0I02A and 0I05, which are sensitive to elliptical asymmetries along u/v($\pm 45^o$) laser table coordinates, Aelli is bounded to be $< 5 \times 10^{-5}$ in RTP and 1.5×10^{-4} in KD*P.

2.7.7 Noise

The best case runs for RTP and KD*P show the RMS of Aelli is $1.5 - 5.5 \times 10^{-3}$ (Fig. 15). These runs were performed at 240Hz flip rate, in linesync octet random mode, and analyzed in the multiplet-tree. The integration widow was 3.96ms to be precise. So an entire octet consists of the integration of 31.68ms of data and so the RMS shown in the multiplet tree is 30Hz-like.

$\sqrt{N}$ scaling indicates

$$m = multiplets$$

$$RMS = RMS_{30Hz}\sqrt{(f/m)/30Hz}$$

The time it takes to reach a particular precision p on Aelli can be calculated as

$$N = (f/m)\tau$$

$$p = RMS/\sqrt{N} = RMS/\sqrt{f\tau/m}$$

$$\tau(p) = (m/f)(RMS/p)^2$$

So for 240Hz, octet, we are 30Hz-like and it takes 3-40minutes to reach a precision of $\pm 2 \times 10^{-5}$ on Aelli depending on the bpm.

References

[1] D.W. Higinbotham, T. Keppel, "2017 Version: Jefferson Lab Hall A Standard Equipment Manual", November 2017

[2] R. Silwal, "Probing the Strangeness Content of the Proton and the Neutron Radius of 208Pb using Parity-Violating Electron Scattering", Ph. D. Thesis, University of Virginia (2012). 38

[3] P. Gueye, "Status of the actual Beam Position Monitors in the Hall C Beamline", December 1995.

[4] P. Zhu et al, "Beam Position Reconstruction for the g2p Experiment in Hall A at Jefferson Lab" *Nuclear Instruments and Methods in Physics Research Section A: Accelerators, Spectrometers, Detectors and Associated Equipment*, Volume 808, 1 February 2016, Pages 1-10.

[5] P. Forck, P. Kowina, and D. Liakin, "Beam Position Monitor", CERN-2009-005, p 187, 2009.

[6] C. Hyde-Wright, L. Todor, G. Laveissiere, "Beam Position Studies for E93050", 1999.